A Sub-Pixel Image Registration Technique with Applications to Defect Detection

Zhen-Hui Hu, Jyh-Shong Ju, and Ming-Hwei Perng

Abstract—This paper presents a useful sub-pixel image registration method using line segments and a sub-pixel edge detector. In this approach, straight line segments are first extracted from gray images at the pixel level before applying the sub-pixel edge detector. Next, all sub-pixel line edges are mapped onto the orientation-distance parameter space to solve for line correspondence between images. Finally, the registration parameters with sub-pixel accuracy are analytically solved via two linear least-square problems. The present approach can be applied to various fields where fast registration with sub-pixel accuracy is required. To illustrate, the present approach is applied to the inspection of printed circuits on a flat panel. Numerical example shows that the present approach is effective and accurate when target images contain a sufficient number of line segments, which is true in many industrial problems.

Keywords—Defect detection, Image registration, Straight line segment, Sub-pixel.

I. INTRODUCTION

IMAGE registration is the process of overlaying two or more images of the same scene with the goal to determine the geometric transformation that aligns the test image with the reference image. It has become a fundamental task of image processing in various applications such as template-based automatic optical inspections (AOI), robot vision and image fusion.

Concerning template-based automatic inspections, a computationally efficient registration method with a very high accuracy is becoming a critical factor in their success due to rapid increase in circuit density and the size of a flat panel. In such industrial applications, defects to be detected are becoming smaller and smaller while the inspection time available for the task of AOI is not increased proportionally. Hence there arises the need of a precise and fast sub-pixel image registration method.

Existing image registration techniques are generally classified into two categories: area-based and feature-based methods [17]. Area-based methods generally require computation of intensity correlation between images. Earlier Fourier-based schemes are only capable of matching translated images by means of the shift property of Fourier transform [10].

Ming-Hwei Perng is with the Department of Power Mechanical Engineering, National Tsing Hua University, Hsinchu, 30043, Taiwan, R. O. C. (phone: +886-3-5742611; fax: +996-3-5722840; e-mail: mhperng@pme.nth.edu.tw).

Zhen-Hui Hu is with the Department of Power Mechanical Engineering, National Tsing Hua University, Hsinchu, 30043, Taiwan, R. O. C.

Jyh-Shong Ju is with the Department of Power Mechanical Engineering, National Tsing Hua University, Hsinchu, 30043, Taiwan, R. O. C.

To account for rotation and scaling, Fourier-Mellin transform is adopted. Rotation and scaling are represented as translations in parameter space and estimated by phase correlation [4]. Keller et al. [9] use the pseudopolar estimation to substantially improve approximations of the polar and log-polar Fourier transforms of an image. In the above approaches, the overall complexity is dominated by FFT operations, and optimized FFT implementations are necessary for a real-time performance. However, as the main drawback of area-based methods, the computational complexity measured by the number of transformation grows rapidly as the required accuracy increases.

In contrast, feature-based methods are computationally simpler and faster. Traditionally, the majority of feature-based registration methods consist of three essential steps: (1)features detection, (2)features matching, and (3)model estimation to result in the relative transformation parameters. In general, distinct objects such as edges, corners, line intersections and closed boundary regions are first detected as features and represented by their representative points, the so called control points or feature points [17]. The second, and the most critical, step is to establish the correspondence between two sets of feature points in the absence of some control points due to defect or partial occlusion. For instance, Stockman *et al.* [15] use line intersections as control points and determine the correspondence between them by means of cluster analysis. However, the locations of feature points are generally sensitive to noise and luminance changes [14]. Accordingly, point features do not fit the need of a precise registration problem.

Line features are more reliable than point features in the problem of precise registration and are generally available in man-made objects. When line features are adopted, the Hough transform can be applied to detect the location and orientation of straight lines [7], and the relative rotation angle between the reference and test images can be obtained by an "angle difference histogram" [6,11]. However, the computational effort based on the Hough transform is too demanding for the task of automatic optical inspections. For cases where registration accuracy is an important concern, an iterative scheme has been proposed at a cost of additional computation effort [6]. Alternatively, the Hausdorff distance and the multi-resolution search of the transformation space [1,16] have also been proposed for image registration using line features. Yi and Camps [16] use the orientation, length and middle point of line segments as matching features. Unfortunately, middle points are not reliable features especially in the presence of occlusion. Similarly, the multi-class technique using the Hausdorff distance may suffer from mismatches due to

World Academy of Science, Engineering and Technology
International Journal of Computer and Information Engineering
Vol:2, No:5, 2008

misclassified pixels [1]. As a result, none of the aforementioned approaches can serve the need of fast and accurate sub-pixel registration.
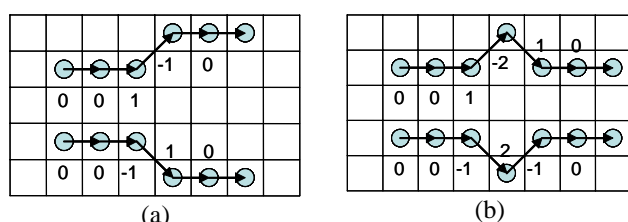

Fig. 1 Chain code difference for straight line segment in two cases. **a** Slanted straight line segment. **b** Shift due to noise

To overcome the aforementioned difficulties in sub-pixel registration, this paper presents a useful method employing a sub-pixel line edge detector [5,13]. In this approach, straight line segments are first extracted from the reference and the test images at the pixel level before applying the sub-pixel edge detector. Next, all sub-pixel line edges are mapped onto the orientation-distance parameter space to solve for the correspondence between line edges in the reference image and those in the test image. Finally, the registration parameters with sub-pixel accuracy are solved via two linear least-square problems. The present approach makes two basic assumptions. First, there are at least two or more groups of parallel line segments with different orientations in the reference and test images. Second, a rigid motion of rotation and translation occurred between these two images, where a small rotation angle is assumed. Many industrial applications conform to these conditions, for example, images of printed circuits.

The rest of this paper is organized as follows. Section 2 presents a three-step process to extract straight line segments as registration features. Section 3 details a two-stage matching procedure to find correct corresponding pairs of line segments between two images. In Sect. 4, two linear least-square problems are then analytically solved to obtain the registration parameters. The application of the present approach to defect detection of printed circuits is reported in Sect. 5 before concluding this paper.

II. EXTRACTION OF SUB-PIXEL REGISTRATION FEATURES

This section describes in details the process of extracting distinctive registration features with sub-pixel accuracy for the proposed method. Under the assumption of rigid motion, the relative distances between parallel line segments are invariant to rotation and translation, which gives significant information for the task of spatially aligning images. Below, straight line segments are first extracted at the pixel level. Then, sub-pixel edge detection is applied at a small cost of additional computations. Finally, the extracted line segments are mapped onto the orientation-distance parameter space for feature matching.

To extract straight line segments at the pixel level, edges are first detected on the reference and test images. Then, edge pixels are traced and linked to form connected paths, from which straight line segments can be acquired. Among those available edge detectors [8], the Sobel operator is adopted in

this paper due to its insensitivity to noise and efficiency in computation. Note that we need to detect only strong edges which do not necessarily form a closed loop, hence there is no need for complex and time consuming edge detectors such as the Canny edge detector [3].

Next, all connected paths are obtained by scanning the edge images using chain code difference [8]. The edge image is scanned from left to right and top to bottom. Every edge point is assigned a chain code difference if one or more 8-connected neighbors [8] exist. The search sequence for the next edge pixel of a connected path is anticlockwise so that the direction of each edge pixel to the next pixel can be uniquely encoded even at branch points. If there are no further 8-connected neighbors, current searching procedure for a connected path ends and we move to the pixel next to the last starting point for a new tracking. In this manner, edge pixels that belong to the same path can be grouped and recorded. A path length threshold is utilized to reject small edge segments and noise.

After then, the chain code differences recorded in each selected path are surfed to determine a straight line segment. Since chain code difference characterizes edge direction, a train of all zero chain code differences manifests a straight line segment, and all straight line segments can be obtained by counting consecutive chain code difference. However, referring to Fig. 1, due to the digitalization of line edges into discrete pixels, both a slanted straight line segment and a temporal shift away should be treated as parts of a straight line segment.

Please also notice that, later steps of the present approach can cope with missing line segments, hence there is no need to find all line segments but only a few. This property contributes to the robustness of the present approaches and save significant computational time in handling details such as noises, weak edges and broken line segments.

In the present approach, the complexity of searching for connected paths is at most $O(N_{ep})$ for an edge image with N_{ep} edge pixels, and that of extracting straight line segments is in the order of $O(n_{cp})$, where n_{cp} denote the number of filtered connected paths. Several well-known methods in the literature for the extraction of straight lines [2,12] can also be used instead of the present procedure. However, the aforementioned procedure is preferable because of its computational simplicity.

The resolution of an imaging device is limited to pixel level only. To achieve a sub-pixel accuracy, a Zernike moment operator [5,13] is adopted in this paper to pin point the sub-pixel locations of the edge points in the previously extracted straight line segments. Consider a simple 2D sub-pixel step edge model as those in [5,13] to parameterize every edge point. A window of size 5×5 pixels is employed to calculate the Zernike moments. The rule of thumb for determining the window size is that it should be large enough to cover the range of intensity changes in the acquired edges to consider the blurring effect of an imaging lens. Due to length limit, details of computation are referred to [5,13]. By means of a few computations, the sub-pixel location parameters for each

World Academy of Science, Engineering and Technology
International Journal of Computer and Information Engineering
Vol:2, No:5, 2008

edge point in the extracted straight line segments can be obtained.

Before line matching and the estimation of transformation parameters, all straight line segments with sub-pixel location accuracy are represented in the polar form $x\cos\theta + y\sin\theta = \rho$. For a given set of edge points in a straight line segment, the parameters (θ_i, ρ_i) can be analytically derived through a least-square fitting [8], and consequently, each straight line segment is mapped onto a point (θ_i, ρ_i) in the $\theta - \rho$ axis, i.e., the Hough space. The merit of using this polar form is stated in the followings.

Parallel straight line segments can be mapped near vertically in the Hough space with very close orientations, which is beneficial in establishing group matching between the reference and test images. For example, as shown in Fig. 2, all line segments are grouped into different sets according to their orientations and then group matching can be easily achieved under the assumption of a small rotation.

Compared to the techniques based upon Hough transformation implementation, the characterization of line segments into the Hough space presented in this section is explicit, precise and efficient since sub-pixel accuracy is realized and no compromise between discrete parameter space and computational complexity exists in determining the point location in the Hough space. In the next section, the advantage of polar form representation will be further exploited.

III. FINDING CORRESPONDING PAIRS OF LINE SEGMENTS

In Sect. 2, straight line segments with sub-pixel accuracy are extracted and characterized into the polar form. Here a two-stage matching technique is proposed to efficiently and robustly find their pair-wise correspondence. In the first stage, the group matching of straight line segments is built based on their orientations. Then line correspondence in matched groups is identified in the second stage by using the relative distance between straight line segments. This matching technique can cope with partial matching if some line segments are missing on account of defects and/or occlusion.

In the following all line segments are first classified into separate groups according to their orientations, then group matching is established by using averaged group orientations. In most potential applications of the present approach such as automatic optical inspection in semiconductor industries, straight line segments are grouped into distinctive clusters, such as $0°$, $45°$, and $90°$. So a simple method like quantization and accumulation of the orientation can be adopted to group those line segments characterized in the Hough space, and then each group can be represented by the average orientations of those line segments in the same group. Accordingly, group matching is achieved if the average group orientations are matched.

Referring to Fig. 2 which illustrates an example of group matching for a sufficiently small rotation, let $G_\theta = \{\bar{\theta}_1, \bar{\theta}_2, \cdots, \bar{\theta}_r\}$ and $G'_\theta = \{\bar{\theta}'_1, \bar{\theta}'_2, \cdots, \bar{\theta}'_s\}$ denote the acquired group orientations in the reference and test images,

respectively, where r and s can be different. Without loss of generality, G_θ and G'_θ are assumed to be strictly ordered, i.e., $\bar{\theta}_{i+1} > \bar{\theta}_i$ and $\bar{\theta}'_{j+1} > \bar{\theta}'_j$. In the present approach, the relative rotation Δ_θ between images is assumed to be sufficiently small such that $\Delta_\theta \ll \Omega_\theta$, where Ω_θ is the minimum orientation difference among all groups, i.e., $\Omega_\theta \triangleq \min\{\min_i\{\bar{\theta}_{i+1} - \bar{\theta}_i\}, \min_j\{\bar{\theta}'_{j+1} - \bar{\theta}'_j\}\}$. Hence it is easy to identify matched group orientations $(\bar{\theta}_i, \bar{\theta}'_j)$ if $|\bar{\theta}_i - \bar{\theta}'_j| < \varepsilon_\theta$, where ε_θ is a matching constant. By sequentially comparing the discriminative group orientations $\bar{\theta}_i$ and $\bar{\theta}'_j$ in G_θ and G'_θ, for $i = 1, 2, \cdots, r$ and $j = 1, 2, \cdots, s$, we can get all matched group orientations $\{(\bar{\theta}_{i1}, \bar{\theta}'_{j1}), (\bar{\theta}_{i2}, \bar{\theta}'_{j2}), \cdots, (\bar{\theta}_{ik}, \bar{\theta}'_{jk})\}$. If two or more pairs of group orientations are matched, then group matching is completed because they are provided with the minimum information for transformation parameter estimation. A simple procedure for this task as listed in Table I will be discussed later. In the following subsection we will proceed to tackle line matching between two matched groups.

TABLE I
A SIMPLE PROCEDURE FOR IDENTIFYING MATCHED DATA PAIR

1.	Set matching constant ε_{MT} and stopping threshold T_{sc}; Reset $T_c = 1; k = 1$
2.	For $i = 1, 2, \cdots, n$ do While $T_c < T_{sc}$ do For $j = k, \ k+1 \cdots, m$ If $|d_i - d'_j| \le \varepsilon_{MT}$, $M(T_c, 1:2) = (i, j)$; $T_c = T_c + 1$; $k = k + 1$

To deal with the problem of line matching depicted in Fig. 2, we will transcribe the original line matching problem into a problem of data matching between two real sets and present a simple solution scheme by taking advantages of the fact that the relative distance between straight line segments are invariant under rotation and translation.

In the end of the previous section, each straight line segment is characterized in polar form. Therefore here we use $P = \{\rho_1, \rho_2, \cdots, \rho_n\}$ and $P' = \{\rho'_1, \rho'_2, \ldots, \rho'_m\}$ to represent two matched groups in the reference and test images, respectively. P and P' are also strictly ordered since we can properly select one with the largest length for those line segments with equal distances to the origin during the process of line segment extraction. Besides, suppose that two baseline segments ρ_b and $\rho'_{b'}$ in P and P' have been determined while the selection of baseline segments will be discussed later. Then the relative distance from each line segment in P and P' to ρ_b and $\rho'_{b'}$ can be calculated to result in two strictly ordered real

World Academy of Science, Engineering and Technology
International Journal of Computer and Information Engineering
Vol:2, No:5, 2008

sets, $D = \{d_i \mid d_i = \rho_i - \rho_b, i = 1, 2, \cdots, n\}$ and $D' = \{d'_i \mid d'_i = \rho'_i - \rho'_{b'}, i = 1, 2, \cdots, m\}$.

Next, a simple comparison procedure for identifying the corresponding pairs of matched elements between two real sets D and D' is presented in Table I. We first set constants ε_{MT} and T_{SC} , and initialize parameters k and T_C . Then, d_i and d'_j in D and D' are compared sequentially to admit their closeness. The data pair (d_i, d'_j) is admitted as matched if $|d_i - d'_j| \leq \varepsilon_{MT}$, where ε_{MT} determines the similarity of two real data. In practice, a counter can be used to count the number of matching pairs and to terminate the procedure when a specified number of matching is achieved. Please notice that a matched data pair (d_i, d'_j) implies that (ρ_i, ρ'_j) is also matched pair of line segments because their relative distances to the baseline segments are nearly the same. As a result, matched line segments in P and P' can be acquired once the data matching between D and D' is completed. Table II is the summary of the proposed algorithm for line matching.

TABLE II
ALGORITHM FOR LINE MATCHING

Step 1.	Determine the baseline segments ρ_b and $\rho'_{b'}$ from P and P' .
Step 2.	Compute the relative distance sets D and D' .
Step 3.	Find matched data pairs M between D and D' using the simple procedure listed in Table I.

Moreover, because the task of line matching is completed when a sufficient number of lines are matched, the above matching procedure can accommodate missing line segments.

The question remains how baseline segments are determined. A workable approach is presented here to find all candidate baselines. Let the relative distance between two neighboring straight line segments in P and P' be denoted as $c_i \triangleq \rho_{i+1} - \rho_i$ and $c'_i \triangleq \rho'_{i+1} - \rho'_i$, respectively, and $C \triangleq \{c_i \mid i = 1, 2, \cdots, n-1\}$, $C' \triangleq \{c'_i \mid i = 1, 2, \cdots, m-1\}$. If the relative distance pair (c_i, c'_j) are taken as nearly equal, i.e., $|c_i - c'_j| \leq \varepsilon_{BT}$, then ρ_i and ρ'_j can serve as a candidate baseline pair. So we scan the relative differences in C and C' , and identify those pairs (c_i, c'_j) with nearly equal relative distance by means of the same comparison procedure listed in Table I, except for another matching constant ε_{BT} for baseline. It should be noted that, if there are n_b candidate baseline segment pairs, then at most n_b matching procedures are required in Table II to establish the correspondence between line segments in P and P' .

IV. ESTIMATION OF TRANSFORMATION PARAMETERS

Once the line correspondence between the reference and test images is established, the present approach proceeds to estimate the transformation parameters discussed in this section.

Under the assumption of a rigid motion, let the transformation parameters be the relative rotation angle Δ_θ and the relative translation (t_x, t_y) and suppose that m corresponding pairs of line segments in total have been identified previously, including the collections from different matched groups. Moreover, let (x_{in}, y_{in}) denotes the nth edge point of the ith matched line segment in the reference image, where (x_{in}, y_{in}) , $i = 1, 2, \cdots, m$, $n = 1, 2, \cdots, n_i$.

In image reconstruction, each registered pixel can be obtained in a backward transformation from the test image using the inverse of the estimated mapping function. Similar ideas can be used to solve for the transformation parameters. Each line segment in the test image can be backward transformed into the reference image to overlay the counterparts by using rotation angle $-\Delta_\theta$ and the relative translation $(-t_x, -t_y)$. In mathematical terms,

$$(x - t_x) \cos(\theta'_i - \Delta_\theta) + (y - t_y) \sin(\theta'_i - \Delta_\theta) = \rho'_i \quad (1)$$

Hence the edge points (x_{in}, y_{in}) in the reference image should satisfy (1) and the following least-square problem is formulated for accurate registration

$$\min_{\Delta_\theta, t_x, t_y} \sum_{i=1}^{m} \sum_{n=1}^{n_i} \left[(x_{in} - t_x) \cos(\theta'_i - \Delta_\theta) + (y_{in} - t_y) \sin(\theta'_i - \Delta_\theta) - \rho'_i \right]^2 \quad (2)$$

Apparently, the above minimization problem (2) is nonlinear in the transformation parameters Δ_θ and (t_x, t_y) , and it requires a computationally intensive optimization solution. In the following we will decouple the nonlinear minimization problem (2) into two linear parts: rotation and translation, respectively. Furthermore, closed-form solutions will be analytically derived.

Noting from (1), the change of the orientation is completely originated from the relative rotation introduced in a rigid motion. Hence, the relative rotation angle Δ_θ can be estimated from backward registration of those matched line segments via the following linear least-square problem

$$\min_{\Delta_\theta} \sum_{i=1}^{m} \left[\theta_i - (\theta'_i - \Delta_\theta) \right]^2 \quad (3)$$

It can easily be shown that the analytical solution to the above problem is

$$\hat{\Delta}_\theta = \left[\sum_{i=1}^{m} (\theta'_i - \theta_i) \right] \Big/ m \quad (4)$$

World Academy of Science, Engineering and Technology
International Journal of Computer and Information Engineering
Vol:2, No:5, 2008

Next, substituting $\hat{\Delta}_\theta$ back into the least-square formulation in (2), the original nonlinear least-square problem reduces to

$$\min_{t_x,t_y} \sum_{i=1}^{m} \sum_{n=1}^{n_i} \left[(x_{in} - t_x)\cos\theta_i'' + (y_{in} - t_y)\sin\theta_i'' - \rho_i' \right]^2 \quad (5)$$

where $\theta_i'' \triangleq \theta_i' - \hat{\Delta}_\theta$. The above minimization problem now is linear in t_x and t_y. Then it is easy to verify that the analytical solution to (5) be

$$\hat{t}_x = (a_{22}b_1 - a_{12}b_2)/(a_{11}a_{22} - a_{12}a_{21}),$$
$$\hat{t}_y = (-a_{21}b_1 + a_{11}b_2)/(a_{11}a_{22} - a_{12}a_{21}) \quad (6)$$

where

$$b_1 = \sum_{i=1}^{m} \sum_{n=1}^{n_i} \left[x_{in}\cos^2\theta_i'' + y_{in}\sin\theta_i''\cos\theta_i'' - \rho_i'\cos\theta_i'' \right]$$
$$b_2 = \sum_{i=1}^{m} \sum_{n=1}^{n_i} \left[x_{in}\sin\theta_i''\cos\theta_i'' + y_{in}\sin^2\theta_i'' - \rho_i'\sin\theta_i'' \right]$$
$$a_{11} = \sum_{i=1}^{m} n_i \cos^2\theta_i'', \qquad a_{12} = \sum_{i=1}^{m} n_i \sin\theta_i''\cos\theta_i''$$
$$a_{21} = a_{12}, \qquad a_{22} = \sum_{i=1}^{m} n_i \sin^2\theta_i'' \quad (7)$$

Please notice that the above estimations of transformation parameters are explicit and efficient once the corresponding pairs of line segment are identified.

V. EXPERIMENTAL RESULTS

In this section the proposed registration method and its usefulness in defect detection are first demonstrated. Then extensive experiments are carried out to quantitatively evaluate the matching accuracy. We also compare its efficiency with Hough transform method in finding straight line segments.

Consider the two gray images shown in Fig. 3a and Fig. 3b, the size of which is 232×222 pixels. Both are taken from an AOI application in LCD panel manufacturing, and the test image contains a mouse-bite defect. After extracting straight line segments, we get 10 and 8 candidates for the reference and test images, respectively, as shown in Fig. 3c and Fig. 3d. Note that some parallel line segments with very close relative distance are omitted from candidate line segments. After line matching, we obtain 8 corresponding pairs of line segments: 4 are close to the vertical direction and the other 4 are close to horizontal direction. The rotation and translation parameters are then calculated according to (4) and (6) as listed in Table III.

Next, difference images are constructed by comparing registered images. To point out defects, we transform the reference image and subtract it from the test image. Using gray level value 30 as a threshold, two binary images are obtained as displayed in Fig. 3e and 3f. It is noted that, though the mouse-bite affect the extraction of candidate line segments, the proposed method still correctly locates it. The comparison of Fig. 3e and 3f also suggests the present sub-pixel based registration method is superior to that based on pixel level detection.

Here we quantitatively measure the matching accuracy of our method by performing extensive experiments. First we consider a reference image of size 156×182 pixels as shown in Fig. 4. A random small rigid motion including a small rotation angle within $\pm 5°$ and a small translation within ± 10 pixels in both directions is employed to transform it into an unregistered test image. Then the proposed registration method is applied to find the registration parameters. In total 1,000 experiments have been carried out and the results are given in Table IV, which shows that the present approach is reliable and accurate. The numbers within parentheses are for pixel-level registration, which are inferior to sub-pixel results. Besides, the computation time for extracting straight line segments and for completing an image registration in each experiment are recorded to be 0.893 seconds and 0.951 seconds, respectively, which shows extracting straight line segments occupies about 94% of the computational cost.

To evaluate the efficiency of the present approach for line segment extraction, it is compared with the Hough transform. Two step sizes in the parameter space of Hough transform are used. Besides, Fig. 3a is adopted as another example for the case with much more edge pixels. The results are compared in Table V, which shows that our approach is much faster than Hough transform with fine parameter resolution in $0.1°$ and 0.1 pixel. All above comparisons are based on coding in the MATLAB environment running on a Pentium 4-1.8GHz PC.

TABLE IV
QUANTITATIVE MEASUREMENT OF REGISTRATION ACCURACY OF THE
PROPOSED METHOD (THE NUMBERS WITHIN PARENTHESES ARE FOR
PIXEL-LEVEL REGISTRATION)

	Max (absolute) deviation	Mean (absolute) deviation	Standard (absolute) deviation
rotation angle (Degrees)	0.260 (0.803)	0.0694 (0.227)	0.0426 (0.131)
X-translation (Pixels)	0.888 (1.094)	0.203 (0.291)	0.170 (0.207)
Y-translation (Pixels)	0.963 (1.516)	0.259 (0.503)	0.201 (0.328)

TABLE V
COMPARISON OF EFFICIENCY IN FINDING STRAIGHT LINE SEGMENTS BETWEEN
OUR METHOD AND HOUGH TRANSFORM METHOD

	The present result	HT with steps $1°$ / 1 pixel	HT with steps $0.1°$ / 0.1 pixel
Averaged time for Fig. 4	0.893 sec	1.684 sec	46.0 sec
Averaged time for Fig. 3a	12.4 sec	2.61 sec	168.7 sec

TABLE III
REGISTRATION RESULTS IN THE DEFECT DETECTION EXAMPLE

	Real parameters	Sub-pixel results	Pixel-level results
Rotation	$-0.6°$	$-0.56°$	$-0.45°$
Translations	(-0.2,-0.1) pixels	(-0.21,-0.13) pixels	(-0.04,-0.21) pixels

World Academy of Science, Engineering and Technology
International Journal of Computer and Information Engineering
Vol:2, No:5, 2008

(a) Reference image   (b) Test image

(c) Matched line segments in a   (d) Matched line segments in b

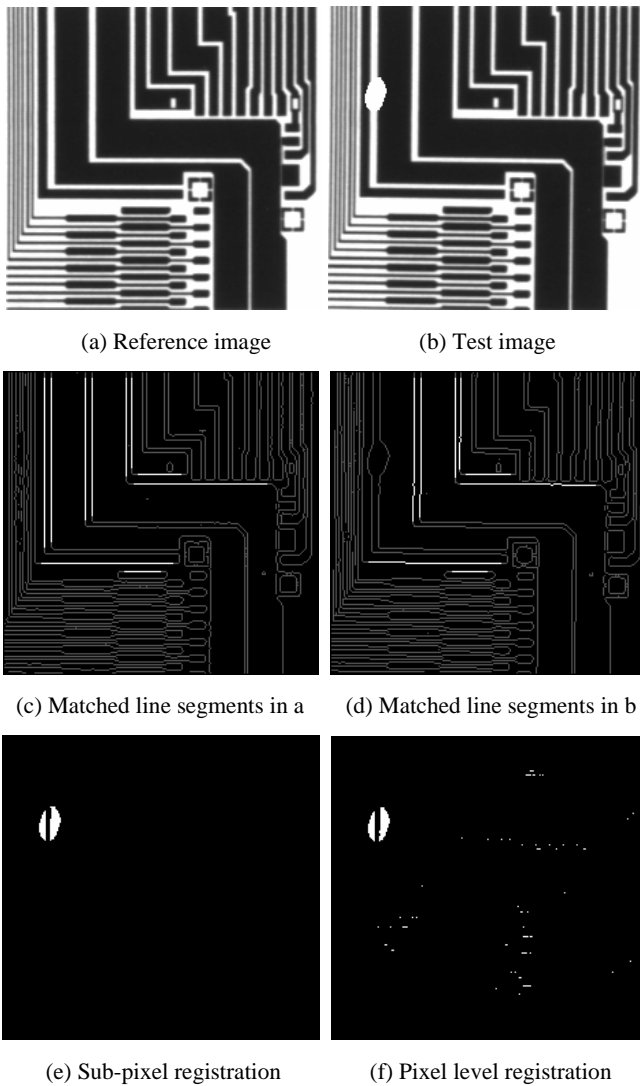(e) Sub-pixel registration   (f) Pixel level registration

Fig. 3 Comparison of defect detection between sub-pixel based
registration and pixel level based registration

a & b: AOI images for registration; c & d : matched line segments;
e & f: binary difference images for gray level threshold value 30

Fig. 4 Synthetic image for evaluating accuracy

VI. CONCLUSION

A practical sub-pixel image registration method using line segments and sub-pixel edge detector has been proposed in this paper. The present approach is computationally efficient, and can be applied to various fields where fast registration with sub-pixel accuracy is required. Numerical example shows that the proposed method is accurate to register images and is suitable for defect detection.

To the knowledge of the authors, the work presented in this paper is the first one in the literature which utilizes the relative distance between parallel line segments as matching features. In comparison with other point-like features or linear features relying on length, center and/or endpoints, the present approach is more reliable, robust and results in more precise registration.

REFERENCES

[1] Alhichri, H. S., Kamel, M.: Multi-resolution image registration using multi-class Hausdorff fraction. Pattern Recognition Letters. **23**, 279-286 (2002).
[2] Burns, J.B., Hanson, A.R.: Extracting straight lines. IEEE Trans. Pattern Anal. Mach. Intell. **4**, 425–456 (1986)
[3] Canny, J.F.: A computational approach to edge detection. IEEE Trans. Pattern Anal. Mach. Intell. **8**(6), 679–698 (1986)
[4] Chen, Q., Defrise, M., Deconinck, F.: Symmetric phase-only matched filtering of Fourier-Mellin transforms for image registration and recognition. IEEE Trans. Pattern Anal. Mach. Intell. **16**(12), 1156-1168 (1994)
[5] Ghosal, S., Mehrotra, R.: Orthogonal moment operators for subpixel edge detection. Pattern Recognition. **26**(2), 295-206 (1993).
[6] Hsieh, J.W., Liao, H.Y.M., Fan, K.C., Ko, M.T., Hung, Y.P.: Image registration using a new edge-based approach. Computer Vision and Image Understanding. **67**(2), 112-130 (1997)
[7] Jain, R., Kasturi, R., Schunck B. G.: Machine Vision. McRraw-Hill (1995
[8] Keller, Y., Averbuch A., Israeli M.: Pseudopolar-based estimation of large translations, rotations, and scalings in images. IEEE Trans. Image Progress. **14**(1), 12–22 (2005)
[9] Kuglin, C. D., Hines, D. C.: The phase correlation image alignment method. In: IEEE 1975 Conf. Cybernetics and Society. pp. 163-165. September (1975)
[10] Li, H. L., Chakrabarti, C.: Motion estimation of two-dimensional objects based on the straight line Hough transform: a new approach. Pattern Recognition. **29**(8), 1245-1258 (1996)
[11] Nevatia, R., Babu, K.R.: Linear feature extraction and description. Comput. Graphics Image Process. **13**, 257–269 (1980)
[12] Qu, Y. D., Cui, C. S., Chen, S. B., Li, J. Q.: A fast subpixel edge detection method using Sobel-Zernike moments operator. Image and Vision Computing, **23**(1), 11-17 (2005).
[13] Shi, W., Shaker, A.: The line-based transformation model (LBTM) for image-to-image registration of high-resolution satellite image data. Int. J.
[14] Remote Sensing. **27**(14), 3002-3023 (2006)
[15] Stockman, G. C. , Kopstein, S., Benett, S.:Matching images to models for registration and object detection via clustering. IEEE Trans. Pattern Anal. Mach. Intell. **4**, 229-241 (1982)
[16] Yi, X., Camps, O. I.: Line-based recognition using a multidimensional Hausdorff distance. IEEE Trans. Pattern Anal. Mach. Intell. **21**(8), 901-916 (1999)
[17] Zitovà, B., Flusser, J.: Image registration methods: a survey. Image and Vision Computing. **21**, 977-1000 (2003).